Hatanaka, Y. Tani, H. Mizuguchi, S. Nakagawa, T. Fujita, A. Yamamoto, Tumor suppressive efficacy through augmentation of tumor-infiltrating immune cells by intratumoral injection of chemokine-expressing adenoviral vector. ***Cancer Gene Ther.***, in press.

11) 杉田敏樹・高 建青・中川晋作; Cell Delivery System を用いた次世代薬物治療: ***Drug Delivery System***、20, 42-48, **2005.**

12) 中川晋作・真弓忠範
細胞性製剤と細胞送達システム(Cell Delivery System)
PHARM TECH JAPAN, 21, 2096-2099, **2005.**

13) 倉知慎之輔・中川晋作
人工改変型ウイルスベクターの現状と今後の展開
遺伝子医学, in press.

G.2. 学会発表

1) Yusuke Eto, Jian-Qing Gao, Shinnosuke Kurachi, Tomohiro Morishige, Hiroyuki Mizuguchi, Yasuo Tsutsumi, Tadanori Mayumi, Shinsaku Nakagawa ; Modification of adenovirus vector with polyethylene glycol enhances accumulation and gene expression in tumor via intravenous injection ; AACR (American Association for Cancer Research) 96th Annual Meeting 2005, 2005 年 4 月, CA, USA

2) 丹羽貴子、吉川友章、小田淳史、飯田恵介、松尾一彦、下川摩里子、岡田直貴、堤 康央、水口裕之、中川晋作; 活性増強変異型抗アポトーシス蛋白質 Bcl-XFNK 発現樹状細胞を用いた腫瘍ワクチン療法; 第 21 回日本 DDS 学会, 2005 年 7 月, 長崎

3) 杉田敏樹、高 建青、金川尚子、本村吉章、飯田恵介、堤 康央、水口裕之、義江 修、真弓忠範、中川晋作; IL-12 及び CCL27 発現アデノウイルスベクターの併用投与による抗腫瘍効果とその有用性評価; 第 21 回日本 DDS 学会, 2005 年 7 月, 長崎

4) 本村吉章、杉田敏樹、高 建青、金川尚子、飯田恵介、堤 康央、水口裕之、義江 修、真弓忠範、中川晋作; IL-12 及び CCL27 発現アデノウイルスベクターの併用投与による抗腫瘍効果増強機構の解明; 第 21 回日本 DDS 学会, 2005 年 7 月, 長崎

5) 金川尚子、杉田敏樹、高 建青、本村吉章、飯田恵介、柳川達也、堤 康央、水口裕之、真弓忠範、中川晋作; IL-12 発現アデノウイルスベクターの腫瘍内投与による抗腫瘍効果と免疫細胞の腫瘍内浸潤; 第 21 回日本 DDS 学会, 2005 年 7 月, 長崎

6) 森重智弘、衛藤佑介、倉知慎之輔、姚 醒蕾、水口裕之、堤 康央、早川堯夫、真弓忠範、中川晋作; ポリエチレングリコール修飾アデノウイルスベクターの EPR 効果に関する検討; 第 21 回日本 DDS 学会, 2005 年 7 月, 長崎

7) Sugita T., Gao J-Q, Kanagawa N., Motomura Y., Nakayama T., Yoshie O., Hatanaka Y., Tani Y., Mizuguchi H., Tsutsumi Y., Nakagawa S. ; Enhanced Anti-Tumor Responses Induced by the Combination of a Couple of Stimulators:IL-12 and CCL27.;The 11th Annual Meeting 2005 The Japan Gene Therapy(第 11 回遺伝子治療学会), Jul., Tokyo.

8) 衛藤佑介、倉知慎之輔、水口裕之、堤 康央、早川堯夫、真弓忠範、中川晋作; 腫瘍ターゲティン

グを目指したバイオコンジュゲート化アデノウイルスベクターの開発;第64回日本癌学会学術総会, 2005年9月, 札幌

9) 岡田直貴、岡田裕香、水口裕之、早川堯夫、中川晋作;腫瘍特異的プロモーターを搭載したファイバー改変型アデノウイルスベクターによるマウスメラノーマ自殺遺伝子治療;第64回日本癌学会学術総会, 2005年9月, 札幌

10) Toshiki Sugita, Jian-Qing Gao, Naoko Kanagawa, Yoshiaki Motomura, Takashi Nakayama, Osamu Yoshie, Yutaka Hatanaka, Yoichi Tani, Hiroyuki Mizuguchi, Yasuo Tsutsumi, Shinsaku Nakagawa ; Synergistic anti-tumor responses induced by the combination of a couple of stimulators: IL-12 and CCL27;第78回日本生化学会大会, 2005年10月, 神戸

11) Ryosuke Koretomo, Naoki Okada, Naoki Mori, Hiroyuki Mizuguchi, Shinsaku Nakagawa, Takuya Fujita and Akira Yamamoto ; Lymphoid tissue directivity and vaccine efficacy of dendritic cells transduced with CCR7 gene by using RGD fiber-mutant adenoviral vector.;20th JSSX-13th NA ISSX Joint Meeting, 2005年10月, Maui, USA

12) Masakazu Niwa, Naoki Okada, Akinori Sasaki, Yutaka Hatanaka, Yoichi Tani, Hiroyuki Mizuguchi, Shinsaku Nakagawa, Takuya Fujita and Akira Yamamoto ; Analysis of immune cell-recruitment and tumor suppressive effect in murine B16BL6 melanoma injected with chemokine-expressing adenoviral vector. ; 20th JSSX-13th NA ISSX Joint Meeting, 2005年10月, Maui, USA

13) 喜田進也、前田光子、北條恵子、衛藤佑介、Jian-Qing Gao、倉知慎之輔、森重智弘、水口裕之、真弓忠範、中川晋作、川崎紘一;アデノウイルスベクター用細胞内移行ペプチドの合成;第55回日本薬学会近畿支部総会・大会, 2005年10月, 西宮

14) 丹羽貴子、吉川友章、小田淳史、飯田恵介、松尾一彦、萱室裕之、岡田直貴、堤 康央、水口裕之、中川晋作;変異型抗アポトーシス蛋白質Bcl-xFNK発現樹状細胞を用いた抗腫瘍効果に関する検討;第35回日本免疫学会総会・学術集会, 2005年12月, 横浜

15) 金川尚子、杉田敏樹、飯田恵介、畑中豊、谷洋一、水口裕之、堤 康央、真弓忠範、中川晋作;IL-12発現ベクターの腫瘍内投与による抗腫瘍効果と免疫系細胞の腫瘍内浸潤の向上;第35回日本免疫学会総会・学術集会, 2005年12月, 横浜

16) 後藤美千代、丹羽貴子、吉川友章、水口裕之、岡田直貴、中川晋作;抗アポトーシス分子を導入した樹状細胞ワクチンの特性と抗腫瘍メカニズムの解析;日本薬剤学会第21年会, 2006年3月, 金沢

17) 森重智弘、衛藤佑介、倉知慎之輔、姚 醒蕾、渡辺 光、岡田裕香、水口裕之、岡田直貴、中川晋作;腫瘍標的化を目指した改良型アデノウイルスベクターの創製;日本薬剤学会第21年会, 2006年3月, 金沢

18) 是友良介、岡田直貴、村上さや香、大西善洋、水口裕之、中川晋作、藤田卓也、山本 昌;アデノウイルスベクターによる樹状細胞の表現型変化とその作用機序に関する基礎的検討;日本薬剤学会第21年会, 2006年3月, 金沢

19) 丹羽正和、岡田直貴、熊谷将成、畑中 豊、谷

洋一、水口裕之、中川晋作、藤田卓也、山本昌;免疫細胞の腫瘍内動員を基盤とした新規癌免疫遺伝子治療の開発;日本薬剤学会第 21 年会, 2006 年 3 月, 金沢

20) 桜井晴奈、櫻井文教、佐々木朋美、川端健二、小泉直也、黄 海瑛、倉知慎之輔、中川晋作、水口裕之;Lipoplex とアデノウイルスベクターの in vivo における遺伝子発現能および自然免疫誘導能の比較;日本薬学会第 126 年会, 2006 年 3 月, 仙台

21) 金川尚子、吉川友章、畑中 豊、谷 洋一、水口裕之、堤 康央、岡田直貴、中川晋作;IL-12 発現ベクターを投与した腫瘍組織における免疫イベントの解析;日本薬学会第126年会, 2006年3月, 仙台

22) 倉知慎之輔、小泉直也、桜井晴奈、櫻井文教、川端健二、中川晋作、早川堯夫、水口裕之;カプシド改変アデノウイルスベクターの作製とその機能性評価;日本薬学会第 126 年会, 2006 年 3 月, 仙台

23) 丹羽貴子、吉川友章、後藤美千代、水口裕之、堤 康央、岡田直貴、中川晋作;アポトーシス抵抗性樹状細胞の創製と抗腫瘍ワクチン機能の評価;日本薬学会第 126 年会, 2006 年 3 月, 仙台

24) 本村吉章、吉川友章、柳川達也、杉田敏樹、水口裕之、堤 康央、岡田直貴、中川晋作;マウス T 細胞への遺伝子導入効率に優れるベクターシステムの探索;日本薬学会第126年会, 2006年3月, 仙台

25) 姚 醒蕾、衛藤佑介、倉知慎之輔、森重智弘、渡辺 光、岡田裕香、水口裕之、堤 康央、岡田直貴、中川晋作;ポリエチレングリコール修飾アデノウイルスベクターを用いた腫瘍標的化自殺遺伝子治療の開発;日本薬学会第 126 年会, 2006 年 3 月, 仙台

26) 上羽美貴、岡田直貴、木村芳伸、郷谷真嗣、藤井 愛、水口裕之、中川晋作、藤田卓也、山本昌;ケモカイン・サイトカイン遺伝子を導入した樹状細胞の創製と抗腫瘍効果の評価;日本薬学会第 126 年会, 2006 年 3 月, 仙台

27) 大西康司、岡田直貴、森川愉香里、水口裕之、中川晋作、藤田卓也、山本 昌;TERT 遺伝子を導入した樹状細胞ワクチンの腫瘍増殖抑制効果;日本薬学会第 126 年会, 2006 年 3 月, 仙台

28) 岡田直貴、中川晋作;免疫細胞の体内動態制御に基づいた癌免疫療法の最適化;日本薬学会第 126 年会, 2006 年 3 月, 仙台

H. 知的財産権の出願・登録状況

H.1. 特許取得

該当事項なし

H.2. 実用新案登録

該当事項なし

Conventional Ad

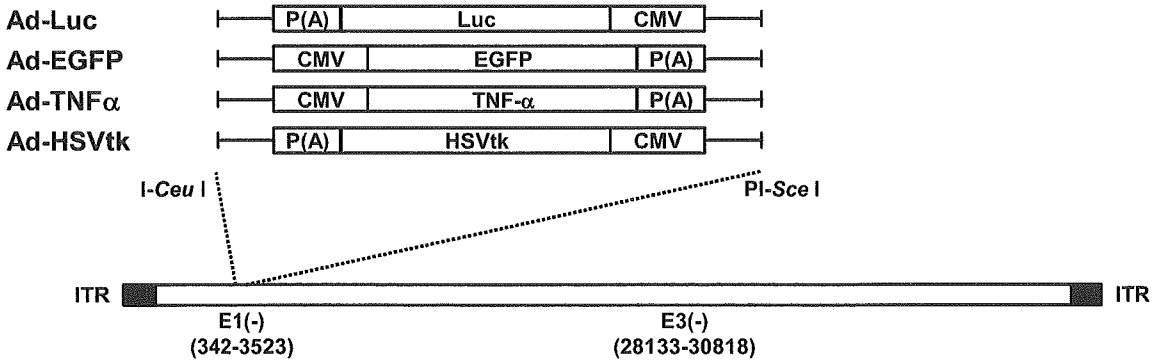

AdRGD

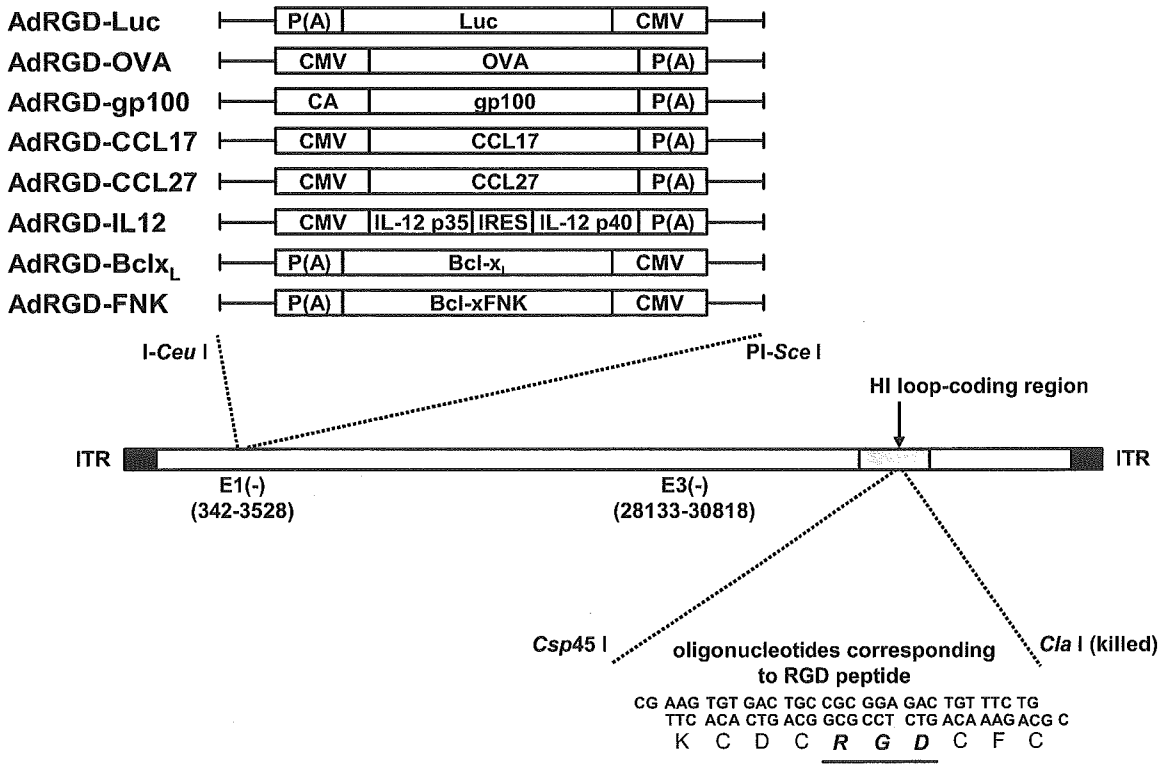

Fig. 1. Schematic representation of conventional Ad and AdRGD used in this study.

Table 1. Primer sequences and reaction parameter used for PCR amplification.

Gene	Primer sequence (5' to 3')	Denaturation	Annealing	Extension	Cycle No.	Product size
Perforin	(F) TTTCGCCTGGTACAAAAACC (R) CAGTCCTGGTTGGTGACCTT	for 30 s at 95°C	for 30 s at 60°C	for 30 s at 72°C	30	680 bp
Granzyme B	(F) CTCGACCCTACATGGCCTTA (R) GAAAGGAAGCACGTTTGGTC	for 30 s at 95°C	for 30 s at 62°C	for 30 s at 72°C	30	507 bp
IFN-γ	(F) GCTTTGCAGCTCTTCCTCAT (R) TGAGCTCATTGAATGCTTGG	for 60 s at 96°C	for 60 s at 50°C	for 60 s at 68°C	30	379 bp
ICAM	(F) CTGGCTGTCACAGAACAGGA (R) AAAGTAGGTGGGGAGGTGCT	for 60 s at 94°C	for 60 s at 54°C	for 60 s at 68°C	30	559 bp
VCAM	(F) CCCAAGGATCCAGAGATTCA (R) TAAGGTGAGGGTGGCATTTC	for 60 s at 94°C	for 60 s at 54°C	for 60 s at 68°C	30	489 bp
β-actin	(F) TGTGATGGTGGGAATGGGTCAG (R) TTTGATGTCACGCACGATTTCC	for 30 s at 95°C	for 30 s at 60°C	for 30 s at 72°C	30	514 bp

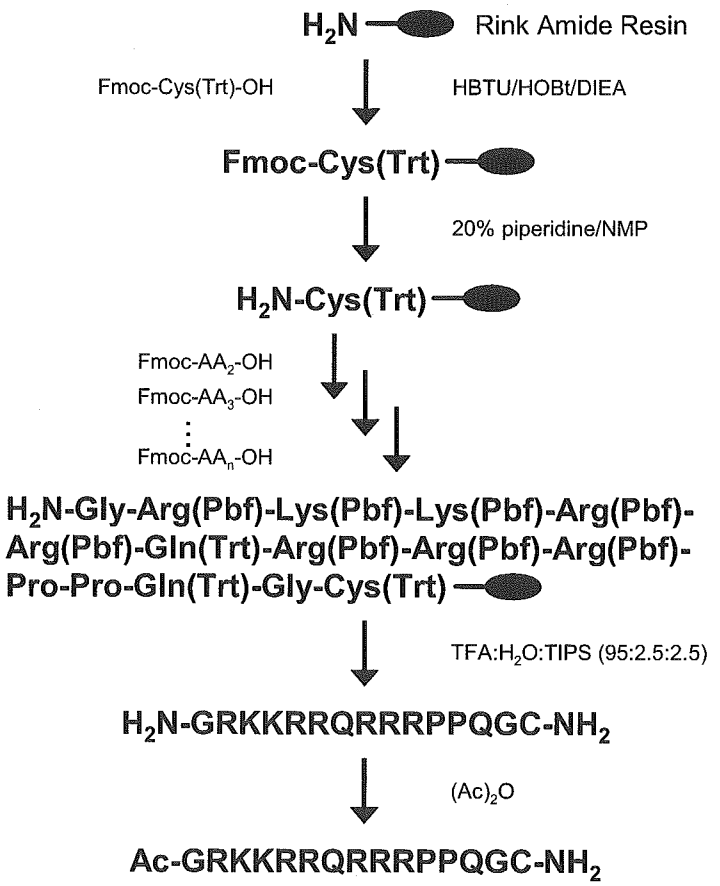

Fig. 2. Structure scheme for Tat peptide.

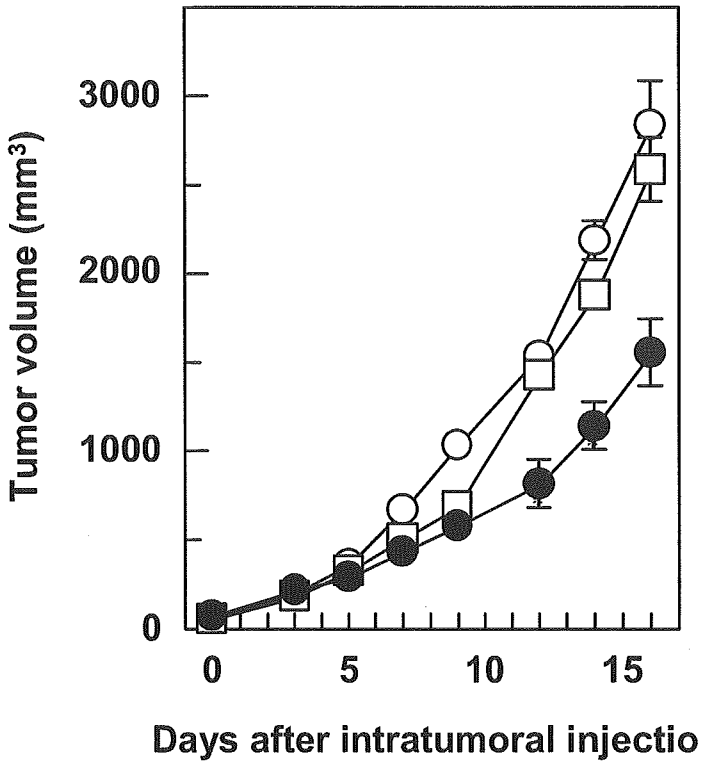

Fig. 3. Anti-B16BL6 tumor efficacy of intratumorally injected AdRGD-CCL17. B16BL6 cells were intradermally inoculated into the right flank of C57BL/6 mice at 4×10^5 cells/mouse. The tumors (5-7 mm in diameter) were injected with AdRGD-CCL17 (●) or AdRGD-Luc (□) at 3×10^8 PFU. Likewise, PBS (○) was injected into the tumors. The tumor volume was calculated after measuring the major and minor axes of the tumor at indicated points. Each point represents the mean ± SE from 6-10 mice.

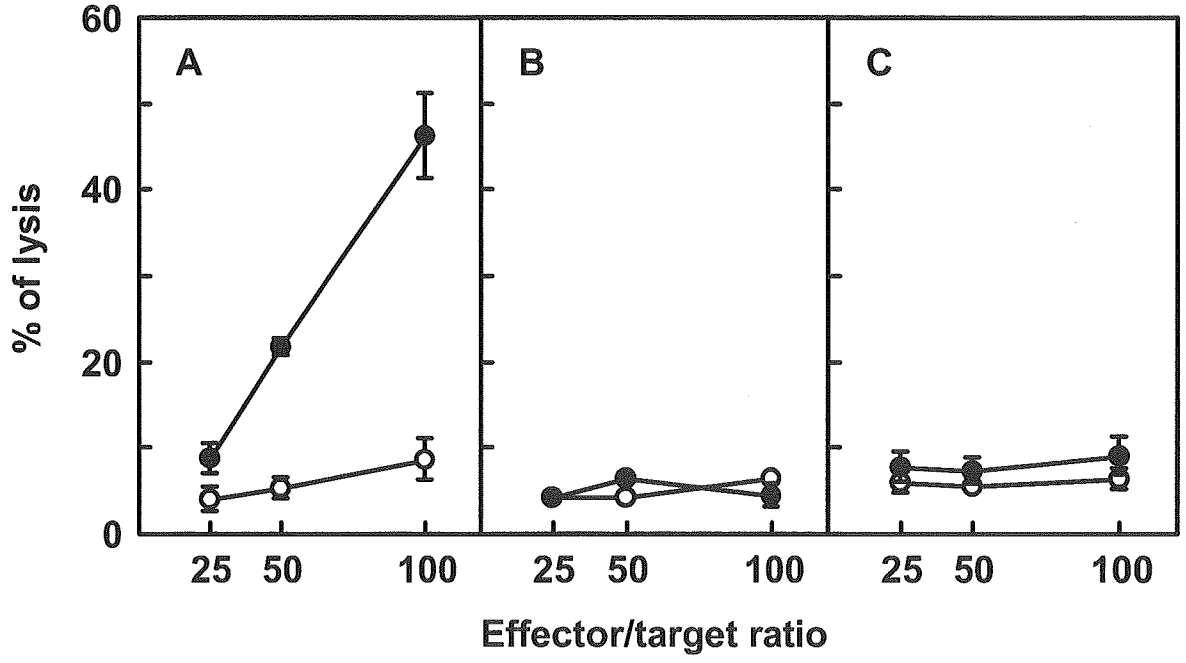

Fig. 4. Enhanced tumor-specific CTL activity in B16BL6 tumor-bearing mice by gp100/DC-immunization. B16BL6 cells were intradermally inoculated into the right flank of C57BL/6 mice at 4×10^5 cells/mouse. One day later, the mice were intradermally injected with 10^6 gp100/DCs (●) or PBS (○) in the left flank. At 1 week after immunization, non-adherent splenocytes were prepared from these mice, and then were re-stimulated *in vitro* for 5 days with IFN-γ-stimulated and mitomycin C-inactivated B16BL6 cells. A cytolytic assay using the re-stimulated splenocytes was performed against IFN-γ-stimulated B16BL6 (A), IFN-γ-stimulated EL4 (B), and YAC-1 (C) cells. The data represent the mean ± SE of three independent cultures from three individual mice.

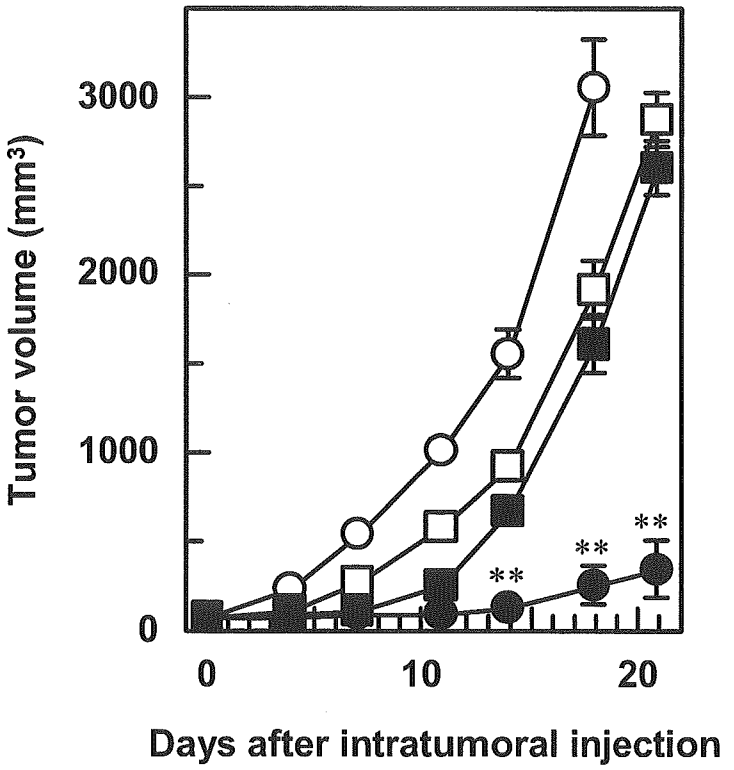

Fig. 5. Anti-B16BL6 tumor efficacy of intratumorally injected AdRGD-CCL17 in combination with gp100/DC-immunization. B16BL6 cells were intradermally inoculated into the right flank of C57BL/6 mice at 4×10^5 cells/mouse. The next day post-tumor inoculation, the mice were intradermally immunized with 10^6 gp100/DCs (●,■,□) or PBS (○) in the left flank. Then, the tumors (5-7 mm in diameter) were injected with AdRGD-CCL17 (●) or AdRGD-Luc (■) at 3×10^8 PFU. Likewise, PBS was administered into control tumors in mice pretreated with gp100/DCs (□) or PBS (○). Tumor volume was calculated after measuring the major and minor axes of the tumor at indicated points. Each point represents the mean ± SE of 7-15 mice. Statistical analysis was carried out by Mann-Whitney *U*-test: *; $p < 0.01$, **; $p < 0.001$ versus AdRGD-Luc-injected group (■).

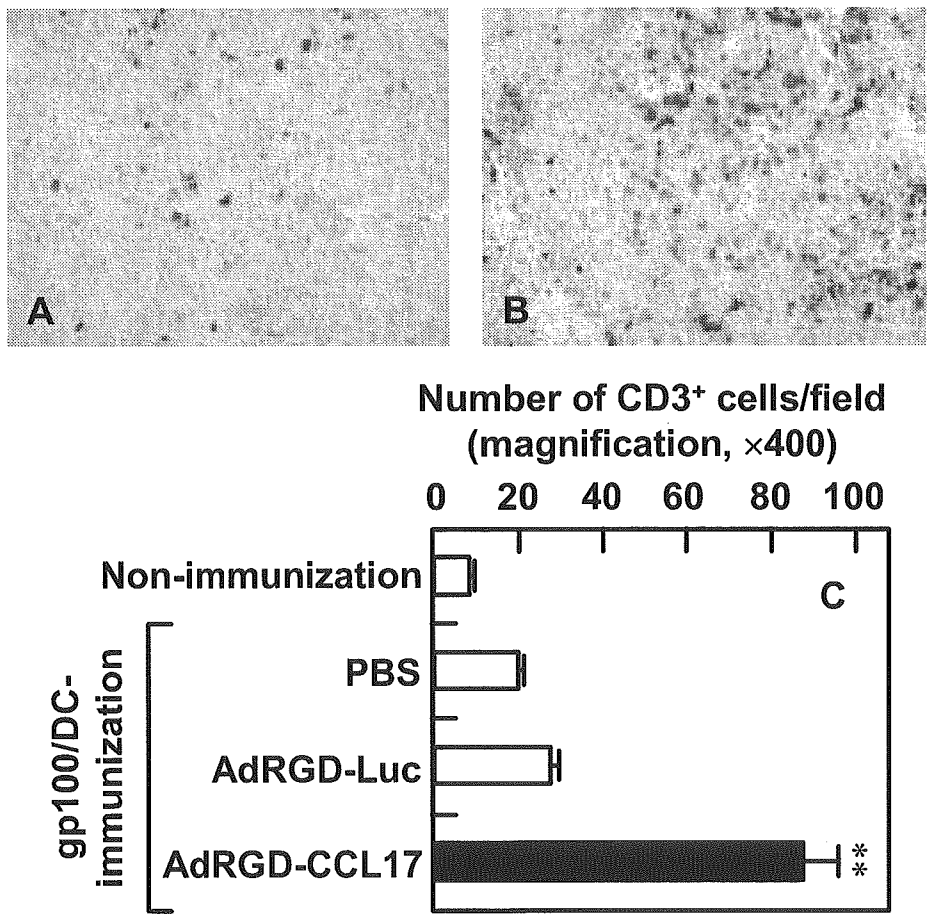

Fig. 6. Infiltration of T cells into B16BL6 tumors of mice treated with the combination of gp100/DC-immunization and intratumoral injection of AdRGD-CCL17. B16BL6 cells were intradermally inoculated into the right flank of C57BL/6 mice at 4×10^5 cells/mouse. The next day, the mice were intradermally injected with 10^6 gp100/DCs in the left flank. Then, the tumors (5-7 mm in diameter) were injected with AdRGD-Luc (A) or AdRGD-CCL17 (B) at 3×10^8 PFU. Likewise, PBS was administered into control tumors. On day 2 after intratumoral injection, immunohistochemical staining against CD3 for determining T cells was performed with frozen tumor sections. A and B; original magnifications are ×200. C; the number of CD3-positive cells in the intratumoral section was assessed by counting six fields per specimen under ×400-magnification. The data represent the mean ± SE of results from three tumors. Statistical analysis was carried out by Welch's *t*-test: **; $p < 0.001$ versus AdRGD-Luc-injected group.

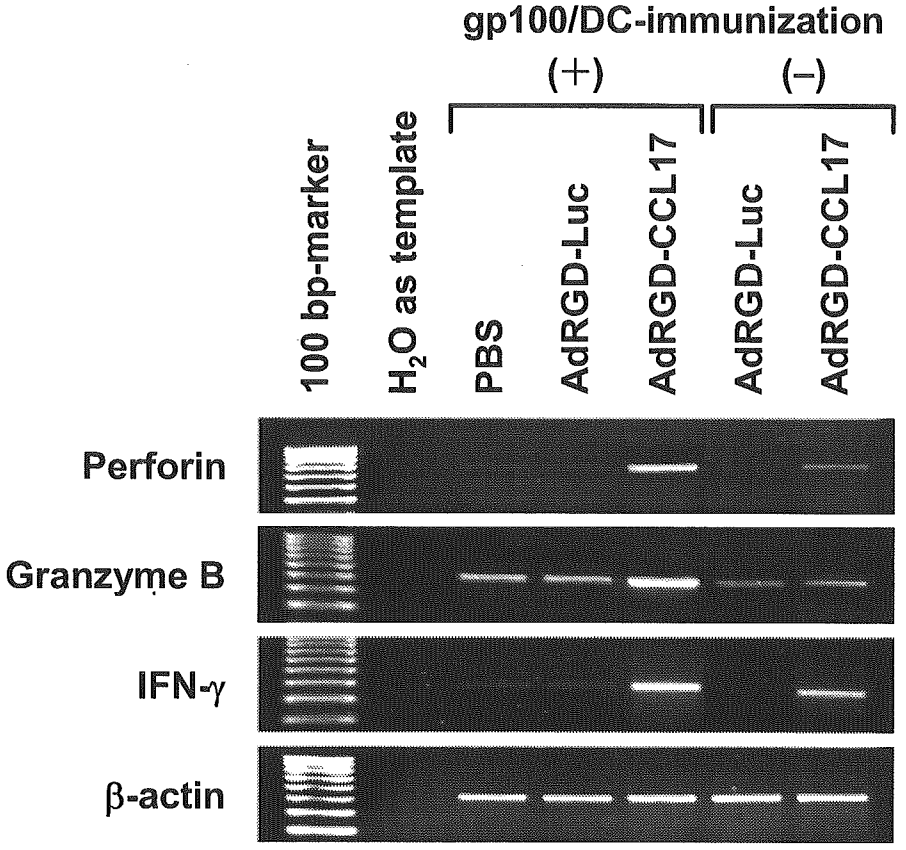

Fig. 7. Activation state of infiltrating immune cells in B16BL6 tumors injected intratumorally with AdRGD-CCL17 in combination with or without gp100/DC-immunization. B16BL6 cells were intradermally inoculated into the right flank of C57BL/6 mice at 4×10^5 cells/mouse. One day later, the mice were intradermally injected with or without 10^6 gp100/DCs in the left flank. The tumor (5-7 mm in diameter) was injected with AdRGD-CCL17 or AdRGD-Luc at 3×10^8 PFU. Likewise, PBS was administered into control tumors. Two days later, total RNA was isolated from the tumors collected from these mice, and then RT-PCR, specific for perforin, granzyme B, and IFN-γ transcripts, was performed. The PCR products were electrophoresed through a 3% agarose gel, stained with ethidium bromide, and visualized under ultraviolet light.

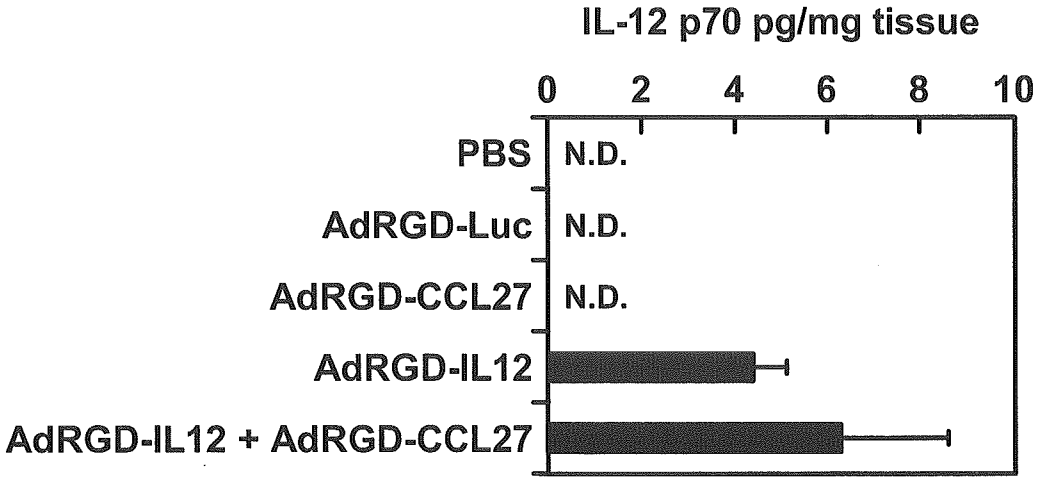

Fig. 8. IL-12 production levels in Meth-A tumors injected with AdRGD-IL12 alone or combined with AdRGD-CCL27. BALB/c mice were intradermally inoculated with 2×10^6 Meth-A cells into the flank. The tumors (9-10 mm in diameter) were injected with AdRGD-Luc alone, AdRGD-CCL27 alone, AdRGD-IL12 alone, or AdRGD-IL12 plus AdRGD-CCL27 in a ratio of 9:1 at the same dose totaling 2×10^7 PFU. PBS was injected into the tumors as a control. Two days later, the tumors were harvested, and then IL-12p70 levels in their homogenates were measured by ELISA. The data represent the mean ± SD of results from three tumors. N.D.: not detectable.

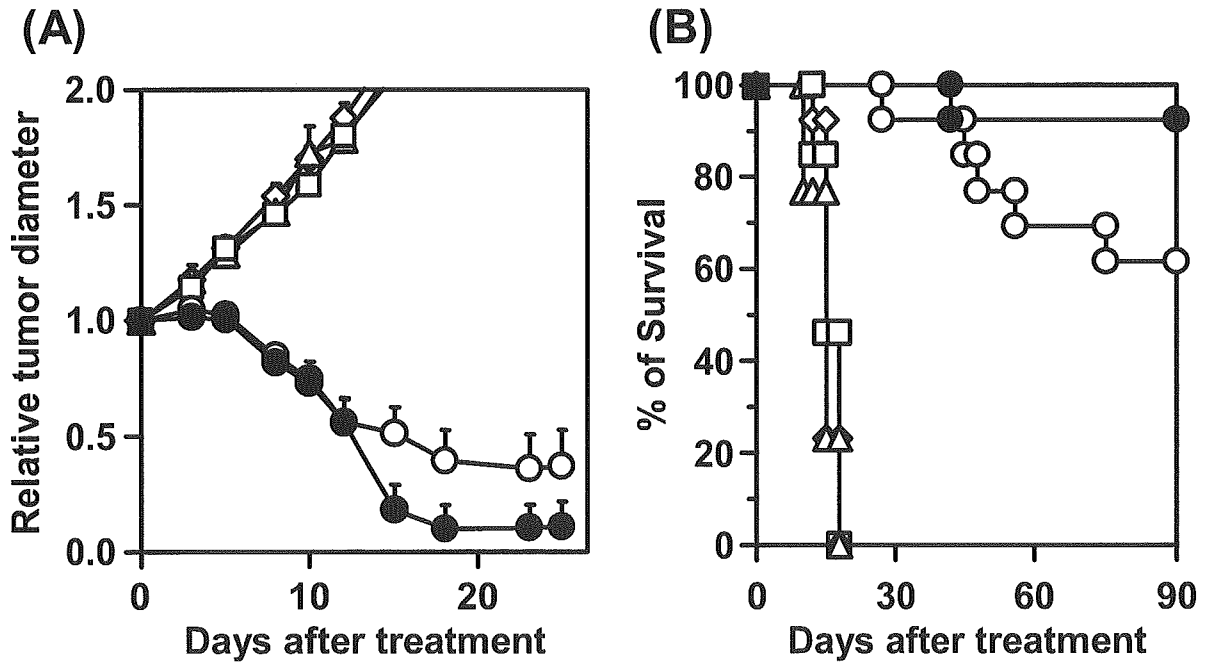

Fig. 9. Antitumor efficacy of intratumorally injected AdRGD-IL-12 plus AdRGD-CCL27 in Meth-A tumor model. BALB/c mice were intradermally inoculated with 2×10^6 Meth-A cells into the flank. The tumors (7-9 mm in diameter) were injected with either AdRGD-Luc alone (△), AdRGD-IL-12 alone (○), AdRGD-CCL27 alone (□), or the combination of AdRGD-IL-12 and AdRGD-CCL27 in a ratio of 9:1 (●) at the same dose totaling 2×10^7 PFU. PBS (◇) was injected into the tumors as a control. (A): The sizes of growing tumors were measured twice a week using microcalipers. Data are expressed as the ratio to the initial tumor diameter. Each point represents the mean ± SE of results from 7 or 8 mice. (B): Data represent the number of mice for which tumors were smaller than 20 mm, expressed as a percentage of the total mice tested in each group.

Table 2. Induction of long-term specific immunity in mice which could achieve complete regression of the primary Meth-A tumor by intratumoral injection with either AdRGD-IL12 alone or the combination of AdRGD-IL12 and AdRGD-CCL27.

Groups	Rechallenging cells[a)]	Tumor-rejected mice/ tested mice
Intact mice	Meth-A	0/10
	CT26	0/5
Meth-A-regressed mice by the injection with AdRGD-IL12	Meth-A	9/9
	CT26	0/6
Meth-A-regressed mice by the injection with AdRGD-IL12 + AdRGD-CCL27	Meth-A	12/12
	CT26	0/5

[a)] Meth-A or CT26 cells were inoculated at 10^6 or 10^5 cells/mouse, respectively.

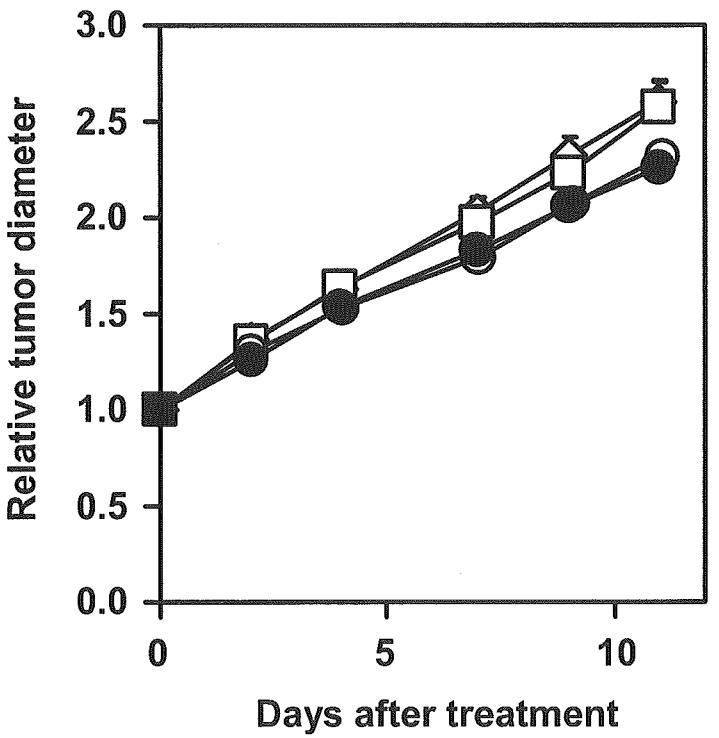

Fig. 10. Growth of Meth-A tumors injected with the AdRGD-IL-12 and AdRGD-CCL27 combination in athymic BALB/c nude mice. BALB/c nude mice were intradermally inoculated with 2×10^6 Meth-A cells into the flanks. The tumors (7-9 mm in diameter) were injected with AdRGD-Luc alone (□), AdRGD-IL12 alone (○), or AdRGD-IL12 plus AdRGD-CCL27 in a ratio of 9:1 (●) at the same dose totaling 2×10^7 PFU. PBS (△) was injected into the tumors as a control. The sizes of growing tumors were measured using microcalipers. Data are expressed as the ratio to the initial tumor diameter. Each point represents the mean ± SE of results from at least six mice.

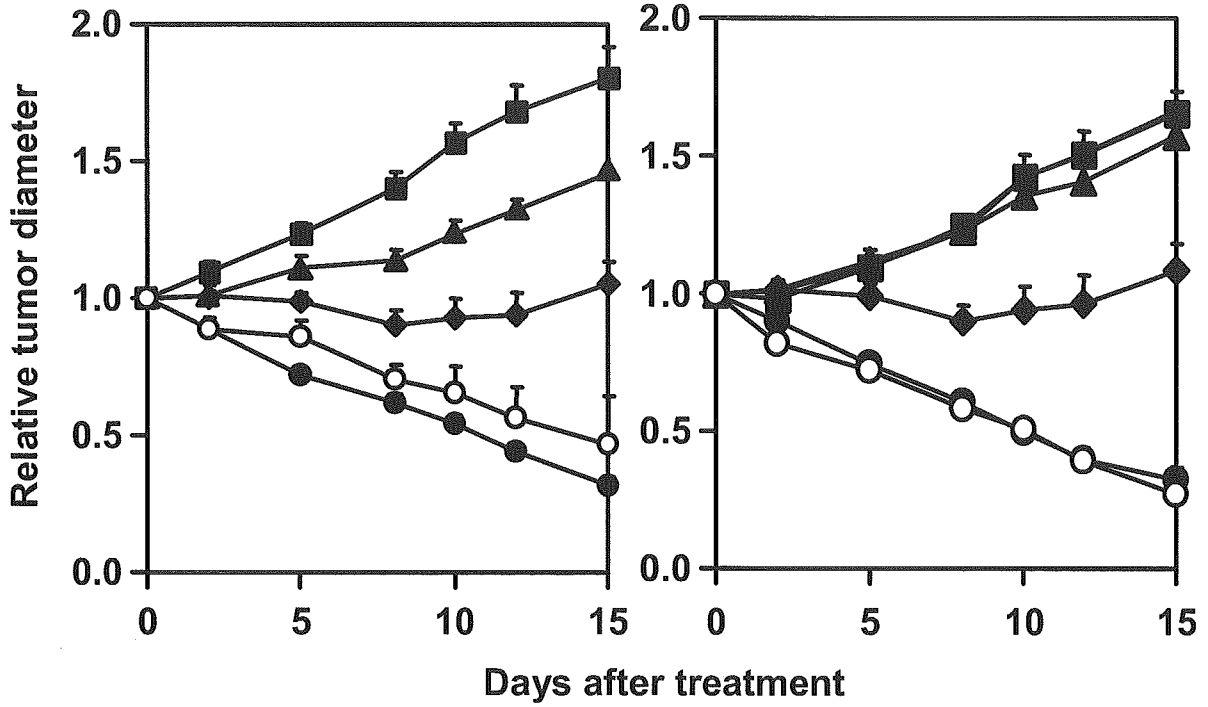

Fig. 11. Determination of immune subsets responsible for the antitumor efficacy induced by the IL-12/CCL27 combination. On day -7, BALB/c mice were intradermally inoculated with 2×10^6 Meth-A cells into the flanks. For depletion of $CD4^+$ T cells (●), $CD8^+$ T cells (▲), or NK cells (◆) in the mice, GK1.5 ascites (anti-CD4), 53-6.72 ascites (anti-CD8), or anti-asialoGM1 antisera were intraperitoneally injected on days -3, -2, -1, 0, 5, 10, and 15. Likewise, for depletion of both $CD4^+$ and $CD8^+$ T cells (■), mice were injected with GK1.5 ascites and 53-6.72 ascites. Normal rat serum (○) was injected into the mice as a control. On day 0, Meth-A tumors received the AdRGD-IL12/AdRGD-CCL27 combination intratumoral injection in a ratio of 9:1 totaling 2×10^7 PFU. Tumor growth was monitored twice a week. Data are expressed as the ratio to the initial tumor diameter. Each point represents the mean ± SE of results from 5-7 mice.

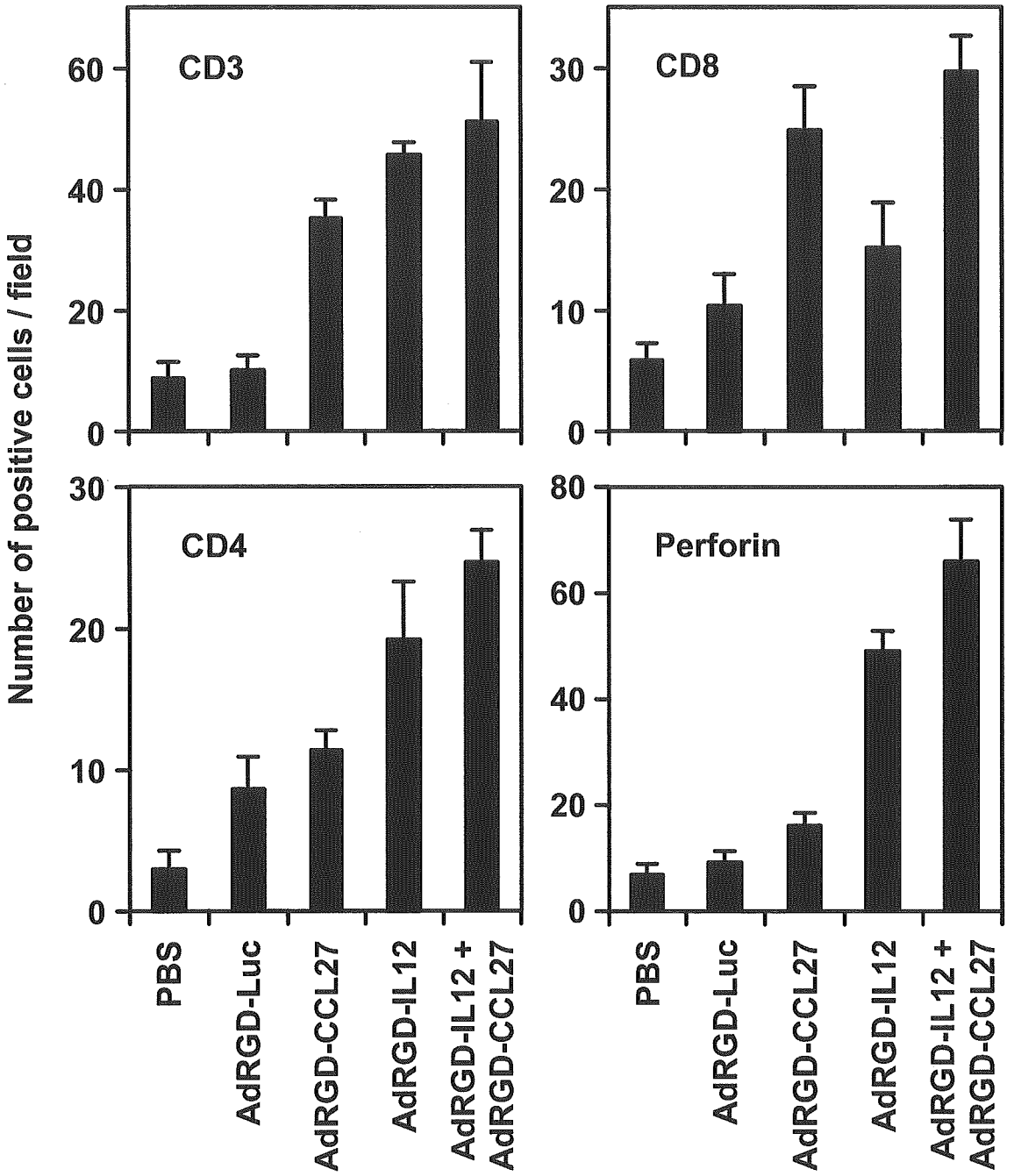

Fig. 12. Quantification of tumor-infiltrating T cell subsets and perforin-positive cells in Meth-A tumors injected with the IL-12/CCL27 combination. Meth-A cells were intradermally inoculated into the flanks of BALB/c mice at 2×10^6 cells/mouse. The tumors (7-9 mm in diameter) were injected with AdRGD-Luc alone, AdRGD-CCL27 alone, AdRGD-IL12 alone, or the AdRGD-IL12 and AdRGD-CCL27 combination in a ratio of 9:1 at the same dose totaling 2×10^7 PFU. PBS was injected into the tumors as a control. On day 6 after the intratumoral injections, immunohistochemical staining against CD3, CD4, and CD8 was performed using frozen tumor sections. These immunohistochemical sections were used to assess the numbers of $CD3^+$, $CD4^+$, $CD8^+$, and $perforin^+$ cells infiltrating into tumor parenchyma by counting six fields per specimen under ×400-magnification. The data represent the mean ± SD of results from three tumors.

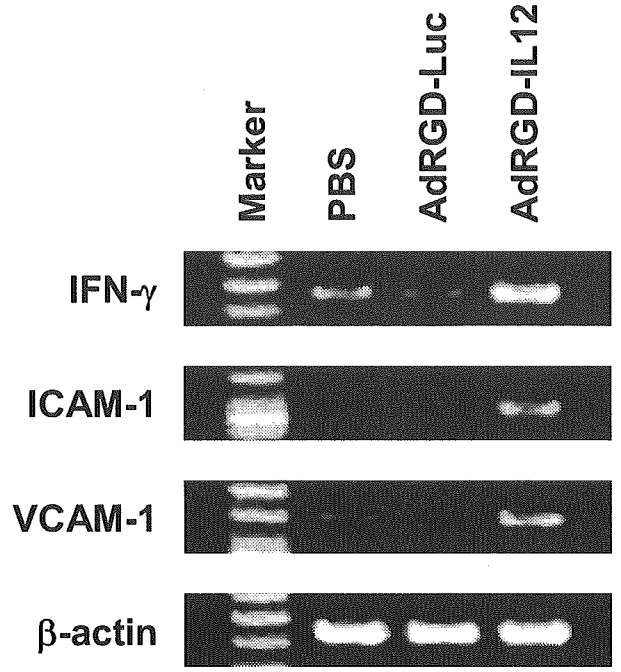

Fig. 13. Increases in expression levels of IFN-γ, ICAM-1, and VCAM-1 in Meth-A tumors injected with AdRGD-IL12. Meth-A cells were intradermally inoculated into the flanks of BALB/c mice at 2×10^6 cells/mouse. The tumors (7-9 mm in diameter) were injected with AdRGD-Luc or AdRGD-IL12 at 2×10^7 PFU. PBS was injected into the tumors as a control. On day 6 after the intratumoral injections, total RNA was isolated from the Meth-A tumors collected from treated mice, and then RT-PCR, specific for IFN-γ, ICAM-1, VCAM-1, and β-actin transcripts, was performed using each primer set descrived in Table 1. The PCR products were electrophoresed through a 2% agarose gel, stained with ethidium bromide, and visualized under ultraviolet light.

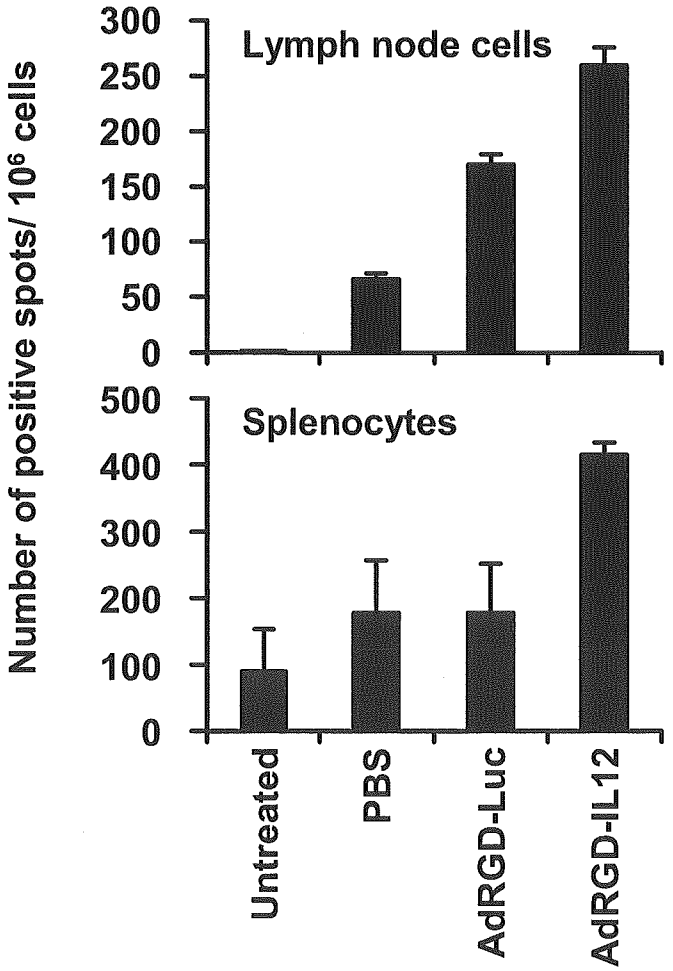

Fig. 14. The frequency of IFN-γ producing cells in draining lymph node cells and splenocytes from Meth-A-bearing mice injected with AdRGD-IL12. BALB/c mice were intradermally inoculated with 2×10^6 Meth-A cells into the flanks. The tumors (7-9 mm in diameter) were injected with AdRGD-Luc or AdRGD-IL12 at 2×10^7 PFU. PBS was injected into the tumors as a control. On day 6 after the intratumoral injections, the draining lymph node cells and splenocytes were prepared from these mice, and then were restimulated *in vitro* with mitomycine C-inactivated Meth-A cells for 24 h. IFN-γ producing cells were evaluated using mouse IFN-γ ELISPOT assay. The data represent the mean ± SE of the results from three mice.

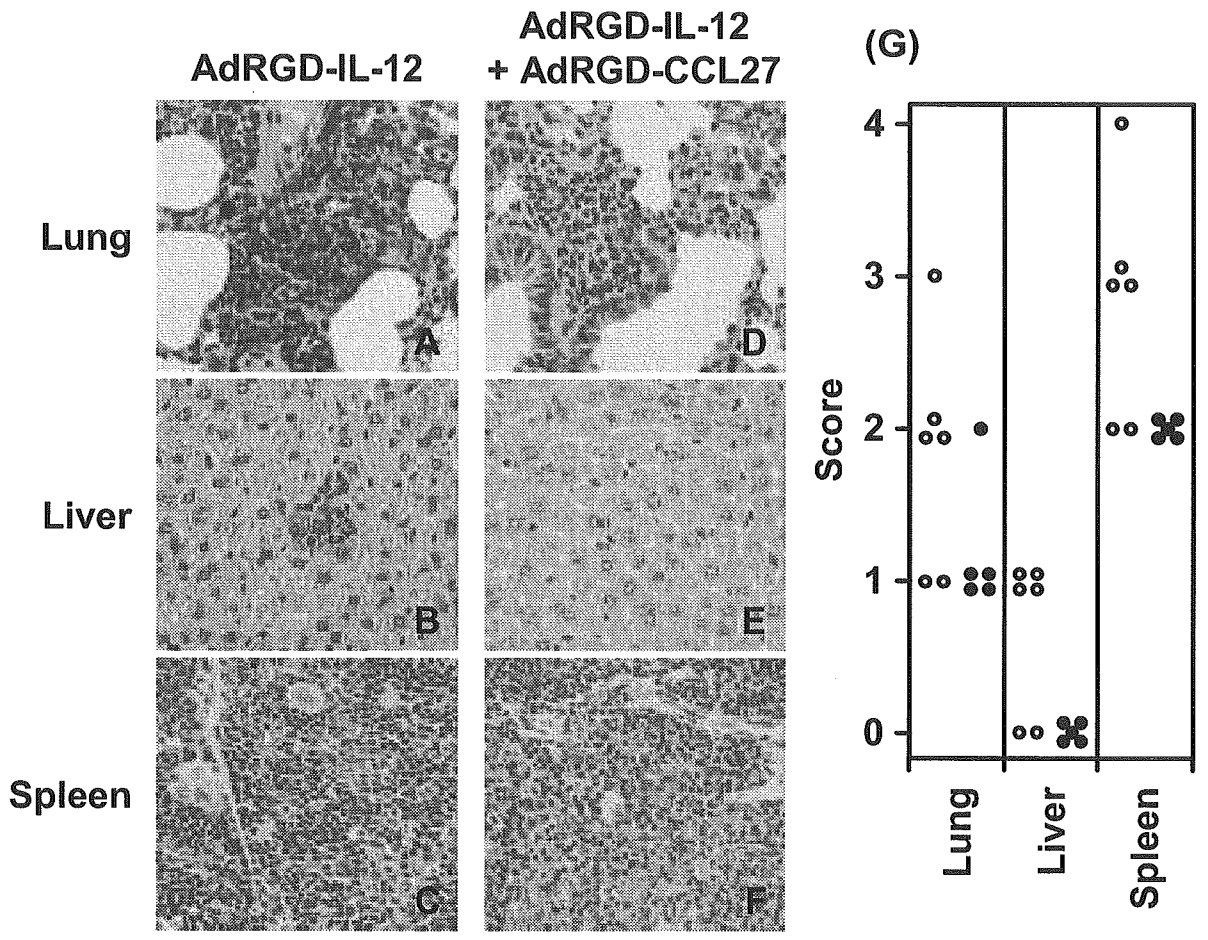

Fig. 15. Histopathological examination of lung, liver, and spleen in Meth-A tumor-bearing mice treated with the AdRGD-IL12/AdRGD-CCL27 combination intratumoral injection. BALB/c mice were intradermally inoculated with 2×10^6 Meth-A cells into the flanks. The tumors (7-9 mm in diameter) were injected with AdRGD-IL12 alone or the AdRGD-IL12 and AdRGD-CCL27 combination in a ratio of 9:1 at the same dose totaling 2×10^7 PFU. Three months later, lung (A and D), liver (B and E), and spleen (C and F) were harvested from mice in which the primary tumors were judged to have completely regressed, and then HE staining was performed using paraffin-embedded tissue sections. Original magnifications are ×300. (G): Histopathological changes (lymphocyte infiltration in lung and extramedullary hematopoiesis in liver and spleen) were scored as: 0, no; 1, rare; 2, mild; 3, moderate; 4, severe. (○); AdRGD-IL12 alone, (●); AdRGD-IL12 plus AdRGD-CCL27.

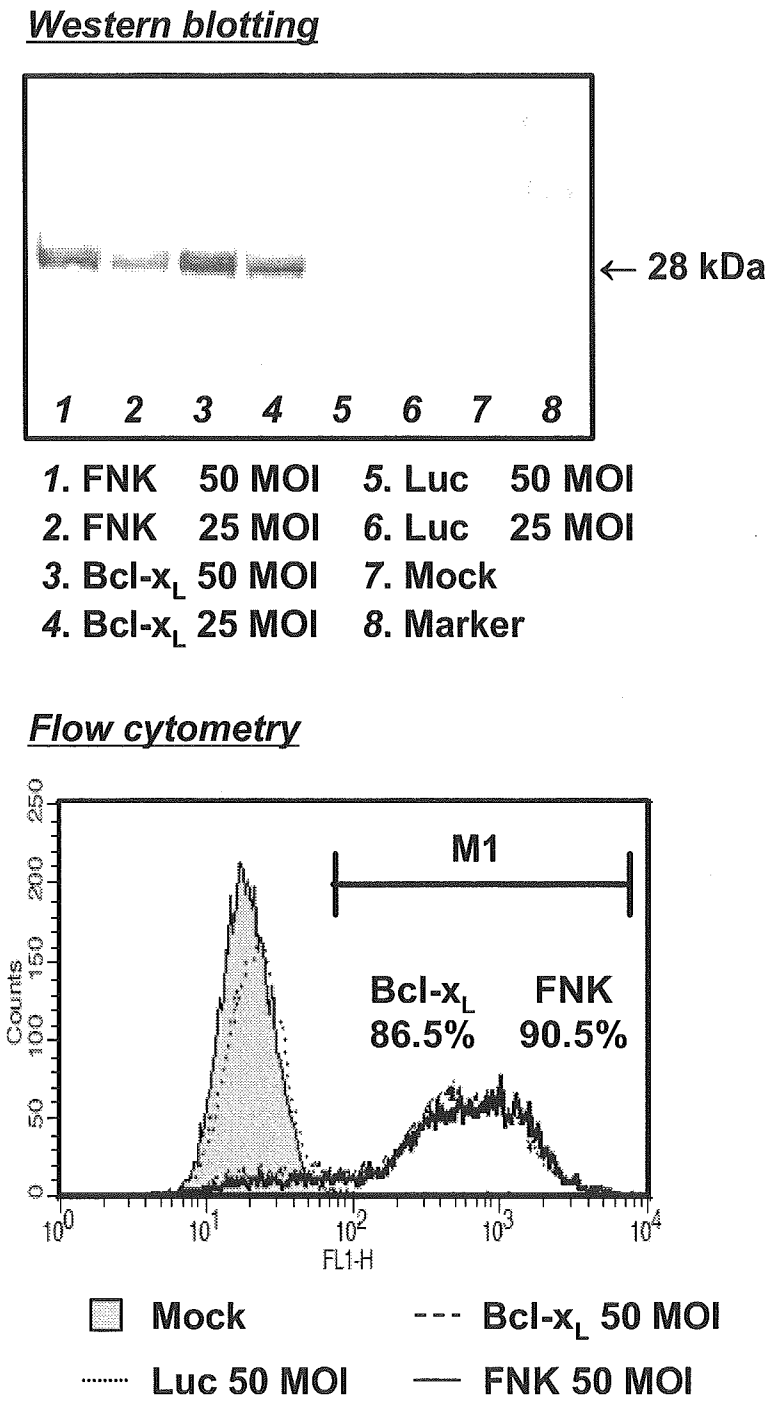

Fig. 16. Gene expression analysis in A549 cells transfected with AdRGD-Bclx$_L$ or AdRGD-FNK. Human A549 cells were transfected with AdRGD-Bclx$_L$, AdRGD-FNK, or AdRGD-Luc at 50 MOI. After 48 h-culutivation, the expression of Bcl-x$_L$ or Bcl-xFNK proteins was assessed by both western blotting and flow cytometry analysis with an intracellular staining method. The % values in the lower panel express the percentage of M1-gated cells.

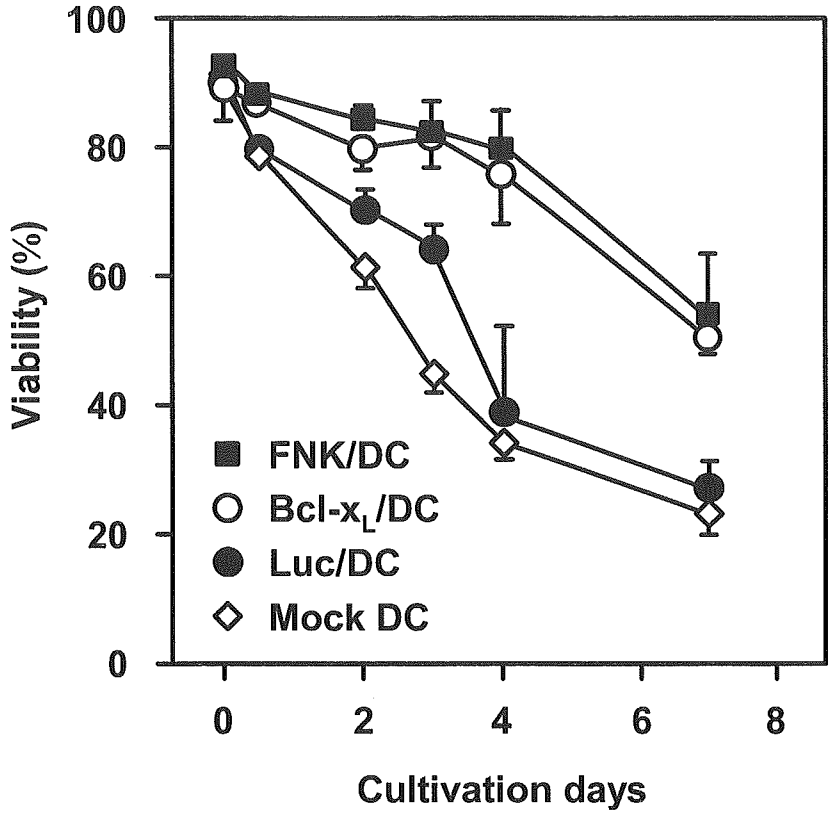

Fig. 17. *In vitro* viability of DCs transfected with AdRGD-Bclx$_L$ or AdRGD-FNK. FNK/DCs, Bcl-x$_L$/DCs, and Luc/DCs were prepared using corresponding vectors at 25 MOI, and then these transduced cells and mock DCs were cultured without cytokines and growth factors. The viability of DCs was assessed by propidium iodide staining at indicated cultivation days. Each point represents the means ± SE of triplicate cultures.

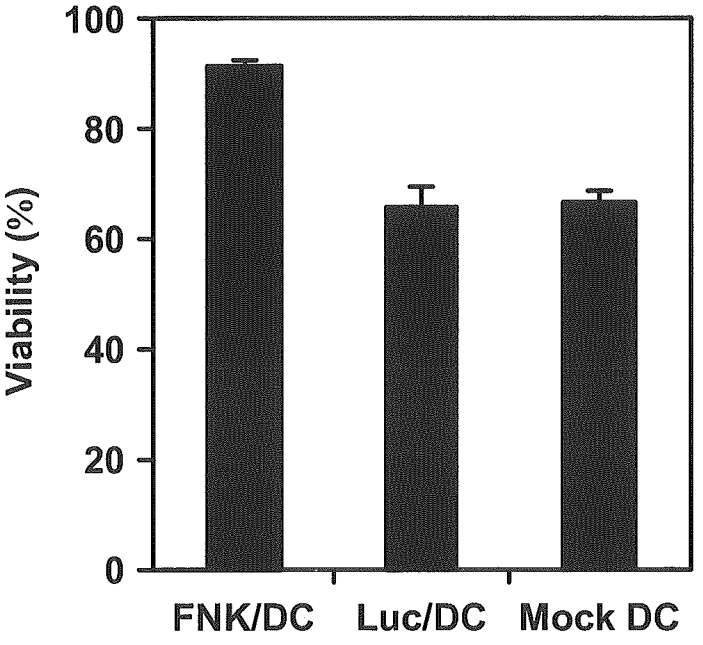

Fig. 18. The resistance of FNK/DCs to apoptosis induced by staurosporine. DCs were transfected with AdRGD-FNK or AdRGD-Luc at 50 MOI. After 48 h-cultivation, the transduced cells were cultured in the presence of 100 nM staurosporine for additional 24 h. The viability was assessed by MTT assay. Data are expressed as means ± SD of triplicate culture.

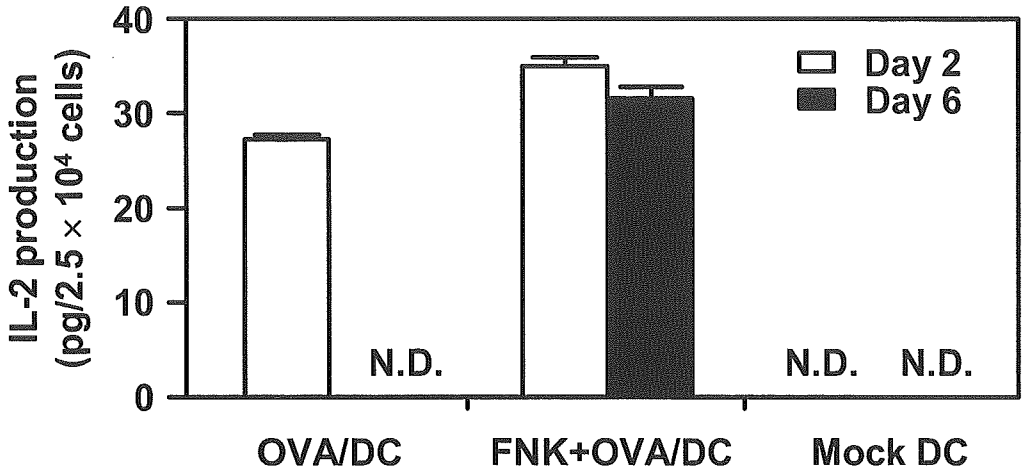

Fig. 19. Duration of antigen presentation in FNK/DCs. DCs were transfected with AdRGD-OVA alone (50 MOI) or the combination of AdRGD-OVA (50 MOI) and AdRGD-FNK (50 MOI) for 2 h. These transduced cells and mock DCs were cultured without cytokines and growth factors. On days 2 and 6, the levels of OVA-peptide presentation via MHC class I molecules on the transduced DCs were determined by bioassay using CD8-OVA1.3 cells. The data represents the means ± SD of three independent cultures. N.D.: IL-2 secreted from CD8-OVA1.3 cells was not detectable.

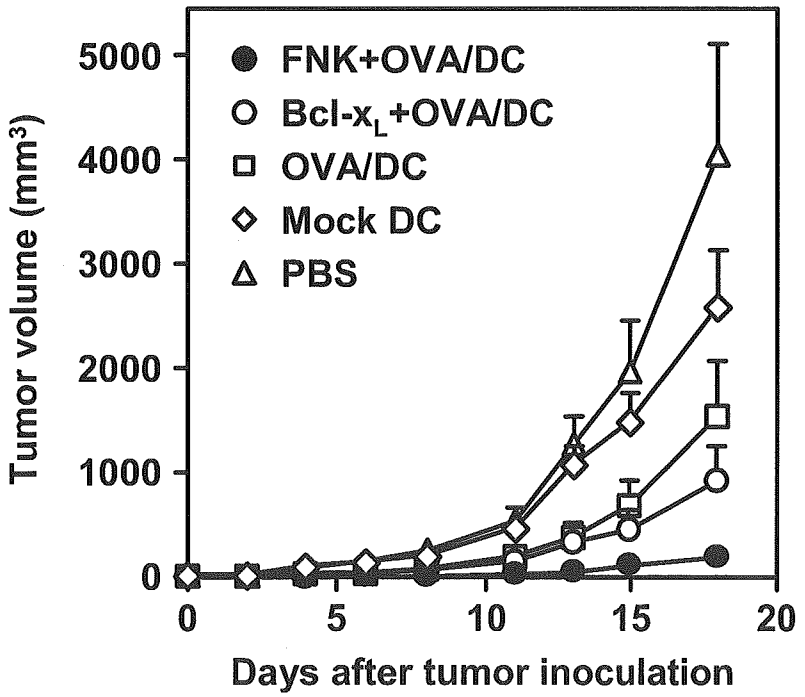

Fig. 20. Vaccine efficacy of DCs co-transduced with OVA gene and either Bcl-x_L or Bcl-xFNK gene against E.G7-OVA challenge. FNK+OVA/DCs, Bcl-x_L+OVA/DCs, and OVA/DCs were prepared using corresponding vectors at 25 MOI, and then cultures for 24 h. C57BL/6 mice were immunized by intradermal injection of transduced DCs into right flank at 5×10^4 cells. One week later, 10^6 E.G7-OVA cells were intradermaly inoculated into the left flank of these mice. The size of tumors was assessed using microcalipers three times per week. Each point represents the mean ± SE from 5-10mice.

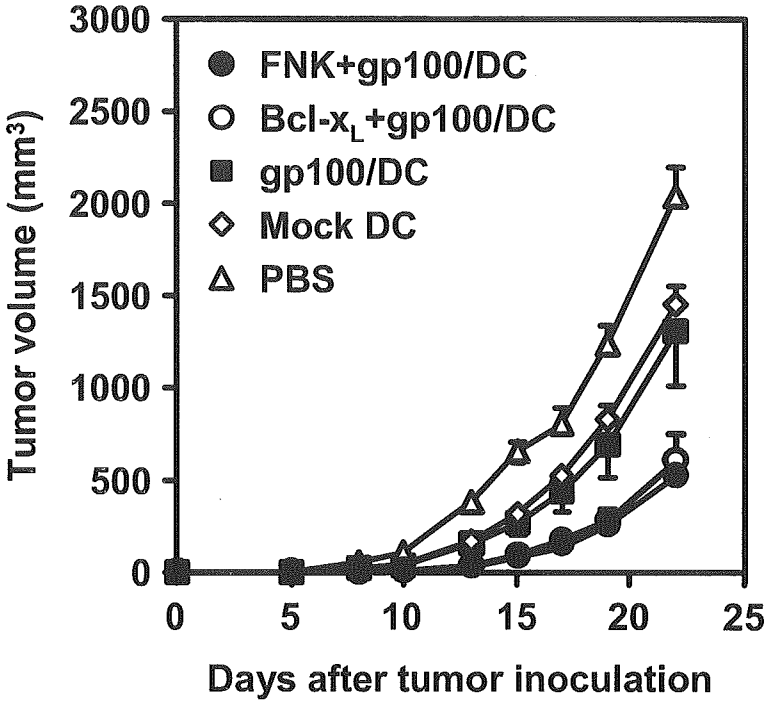

Fig. 21. Vaccine efficacy of DCs co-transduced with gp100 gene and either Bcl-x_L or Bcl-xFNK gene against B16BL6 challenge. FNK+gp100/DCs, Bcl-x_L+gp100/DCs, and gp100/DCs were prepared using corresponding vectors at 25 MOI, and then cultures for 24 h. C57BL/6 mice were immunized by intradermal injection of transduced DCs into right flank at 1.5×10^6 cells. One week later, 5×10^4 B16BL6 cells were intradermaly inoculated into the left flank of these mice. The size of tumors was assessed using microcalipers three times per week. Each point represents the mean ± SE from 5-10mice.

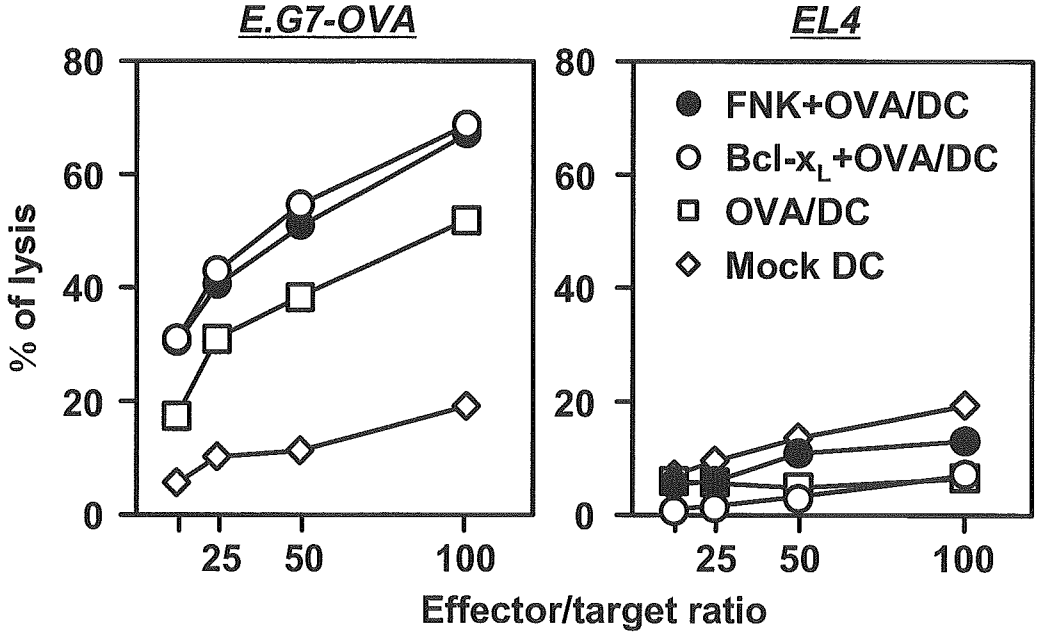

Fig. 22. OVA-specific CTL response in mice immunized with DCs cotransduced with OVA gene and either Bcl-x_L or Bcl-xFNK gene. FNK+OVA/DCs, Bcl-x_L+OVA/DCs, and OVA/DCs were prepared using corresponding vectors at 25 MOI, and then culture for 24 h. These transduced cells and mock DCs were vaccinated once intradermally into C57BL/6 mice at 2.5×10^4 cells. At 1 week after immunization, splenocytes were prepared from these mice, and were re-stimulated *in vitro* for 5 days with mitomycine C-inactivated E.G7-OVA cells. Cytolytic effects of re-stimulated splenocytes (effector cells) against E.G7-OVA or EL4 cells (target cells) were evaluated by ^{51}Cr-release assay.

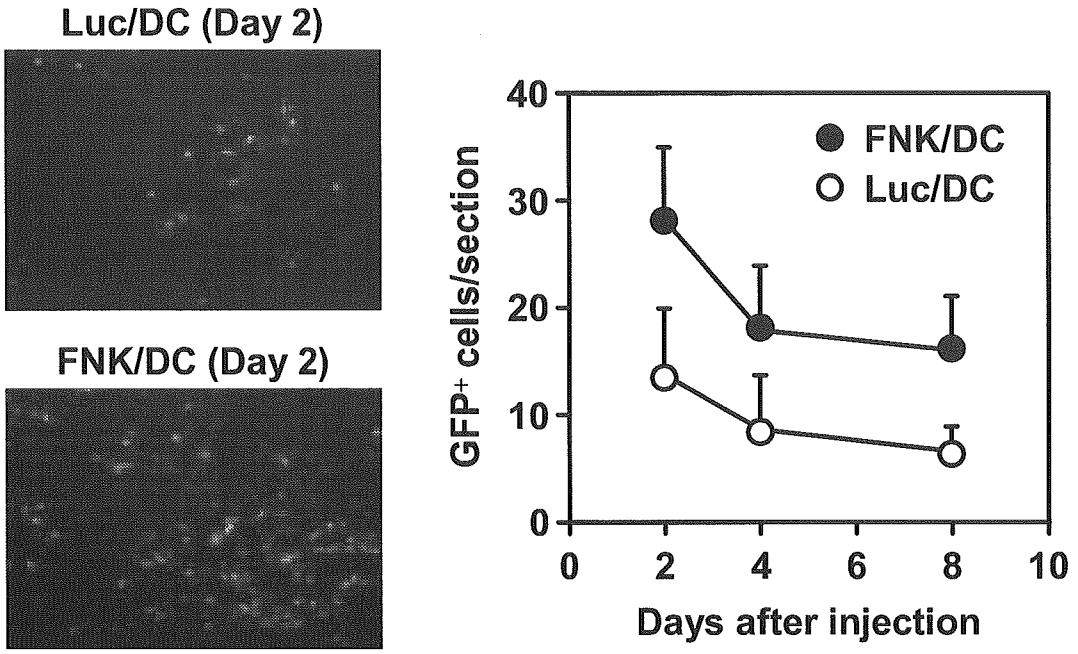

Fig. 23. Enhanced accumulation of FNK/DCs from administration site to regional lymph node. DCs derived from GFP transgenic mice were transfected with AdRGD-FNK or AdRGD-Luc at 25 MOI, and then were cultured for 24 h. These transduced GFP^+ DCs were injected intradermally into right flank of wild type C57BL/6 mice at 2×10^6 cells. The draining inguinal lymph nodes were harvested on days 2, 4, and 6 after injection. Frozen sections (6-μm thickness) of lymph node were prepared, and then the number of GFP^+ DCs was counted under fluorescence microscopy. Each point represents the mean ± SE of results from three mice.

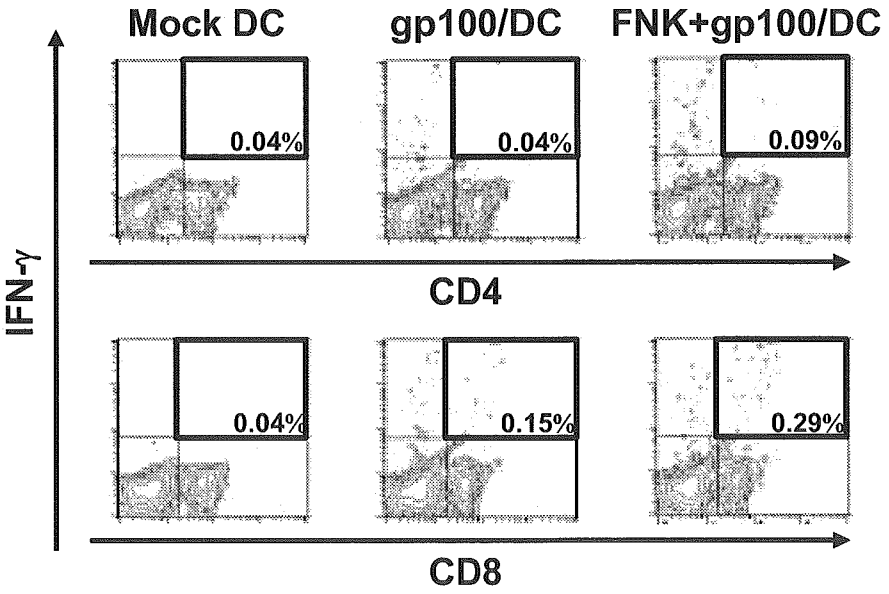

Fig. 24. gp100-specific $CD4^+$ or $CD8^+$ T cell immune response in mice immunized with DCs cotransduced with gp100 and Bcl-xFNK genes. gp100/DCs and FNK+gp100/DCs were prepared using corresponding vectors at 25 MOI, and then culture for 24 h. These transduced cells and mock DCs were vaccinated once intradermally into C57BL/6 mice at 1.5×10^6 cells. At 1 week after immunization, regional lymph node cells were prepared from these mice, and were re-stimulated *in vitro* with mitomycine C- inactivated B16BL6 cells for 24 h. The number of IFN-γ-producing $CD4^+$ or $CD8^+$ T cells was analyzed by intracellular IFN-γ staining followed by flow cytometry.